

Features of the transformation of Hg^{II} by heterogeneous photocatalysis over TiO_2

Silvia G. Botta^a, Diana J. Rodríguez^a, Ana G. Leyva^b, Marta I. Litter^{a,*}

^a Comisión Nacional de Energía Atómica, Unidad de Actividad Química, Av. Gral. Paz 1499, 1650 Buenos Aires, Argentina

^b Comisión Nacional de Energía Atómica, Unidad de Actividad Física, Av. Gral. Paz 1499, 1650 Buenos Aires, Argentina

Abstract

UV/ TiO_2 photocatalysis of 0.5 mM mercuric aqueous solutions has been analyzed starting from $\text{Hg}(\text{NO}_3)_2$, $\text{Hg}(\text{ClO}_4)_2$ and HgCl_2 at different pH (3, 7 and 11) and in the presence or absence of oxygen. Profiles of Hg^{II} concentration with time were characterized by a relatively rapid initial conversion followed by a decrease or an arrest of the rate, the shape of profiles changing with the conditions. Conversions at 60 min and initial quantum efficiencies have been found dependent on the initial conditions and type of mercuric salt. The faster transformation took place at pH 11 for all salts. A good transformation yield is observed also for HgCl_2 , which behaves differently to the other two salts, at pH 3 under nitrogen and pH 7 (N_2 or O_2). Inhibition by oxygen was observed in acid and neutral media but not at basic pH. When the conversion was 50% or more, pale or dark gray solids were deposited on the catalyst, identified as mixtures of Hg^0 , HgO or Hg_2Cl_2 . A unique kinetic scheme could not be defined, which seemed to depend on the nature of the mercury salt, the ambient conditions and the type of deposit. Implications of the application of the technique to real systems are discussed.

© 2002 Elsevier Science B.V. All rights reserved.

Keywords: Mercury(II); TiO_2 ; Heterogeneous photocatalysis

1. Introduction

Heterogeneous photocatalysis (HP) over TiO_2 has been widely used for destruction of organic pollutants in waste waters. Less studied but not less important from the environmental point of view is the photocatalytic transformation of metal ions by oxidation or reduction to species of lower toxicity or easier to separate from the aqueous phase [1–4].

Mercury(II) is a frequent component of industrial waste waters, remarkably toxic at concentrations higher than 0.005 ppm and included in the list of priority pollutants of the US EPA [1], with a disposal limit

of 200 ppb [5]. The major use of mercury compounds is in agricultural applications, taking part of pesticides, fungicides, herbicides, insecticides and bactericides. It is also used in the chlorine-alkali industry, in paints, as a catalyst in metallurgical, pharmaceutical, chemical and petrochemical industries, in electronics, cosmetics, thermometers, gauges, batteries and dental materials. This wide application contributes to the dispersion of the element as a hazardous pollutant. In addition, organic mercury compounds (e.g., methyl- or phenylmercury), which are the most used in agriculture, are considerably more toxic than the inorganic analogous.

Mercuric species in solution cannot be bio- or chemically degraded. Common remediation treatments are precipitation as sulfide, ion exchange, adsorption, coagulation and reduction [4]. HP has been

* Corresponding author. Tel.: +54-116-772-7016;
fax: +54-116-772-7121/7886.
E-mail address: litter@cnea.gov.ar (M.I. Litter).

proposed as a convenient tool for the treatment of mercury in aqueous waste waters [1,2]. In fact, due to the complicated chemistry of mercury in solution and in solid phase, HP processes have not been completely understood. First evidences of heterogeneous photocatalytic transformation of Hg^{II} appeared in 1978, when Clechet et al. [6] photoreduced mercuric salts on a TiO_2 electrode, obtaining calomel or metallic Hg depending on the nature and concentration of the starting salt. Some years before, catalyzed photooxidation of metallic mercury on TiO_2 powders has been also reported, HgO being identified as the reaction product [7].

Later, other works with TiO_2 [4,5,8–18], ZnO [19,20] and pure and modified WO_3 [12,21,22] have revealed additional characteristics of the photocatalytic transformation of Hg^{II} . In most cases, deposition of metallic mercury was reported, although other type of deposits have been informed, their nature being controversial and dependent on the initial conditions [5,6,13,17–20,22,23]. Oxygen inhibited the reaction [4,8–14,16,17,19,20]; deoxygenated conditions produced partial deposition, whereas complete deposition without oxygen was only possible in the presence of a reducing agent as methanol, ethanol or other organics [8,13,14,16,20]. Solar illumination experiments indicated a high efficiency for mercury(II) removal [6,14,19–22]. Cyanide mercuric species [24], citrate complexes [25] and organometallic forms such as methylmercury and phenylmercury(II) [4,10,14] have been also investigated.

In this paper, photocatalytic studies of Hg^{II} transformation, starting from three different inorganic salts are presented. The efficiency of conversion and the nature of the reaction products, together with the influence of variables such as pH and oxygen have been analyzed. A major interest was put to investigate the effect of the nature of the mercury salt (anion type) and of the derived deposit, previously ignored in most of the published works.

2. Experimental

2.1. Chemicals

TiO_2 (Degussa P-25) was provided by Degussa AG Germany and used as received. $\text{Hg}(\text{NO}_3)_2$ (Merck),

HgCl_2 (Bronfield) and $\text{Hg}(\text{ClO}_4)_2$ (Aldrich) of the highest purity were used. All other reagents were at least of reagent grade and used without further purification.

Water was double distilled in a quartz apparatus. Diluted HClO_4 and NaOH were used for pH adjustments.

2.2. Photocatalytic experiments

Irradiations were performed using a high-pressure xenon arc lamp (Osram XBO, 150 W) with a band-pass filter (Schott BG 1 or BG 25, thickness 3 mm; $300 \text{ nm} < \lambda < 500 \text{ nm}$; maximum transmission at 360 nm). The IR fraction of the incident light was removed by a suitable filter (Schott KG 5). Actinometric measurements were performed by the ferrioxalate method [26]. A photon flow per unit volume of $1.1 \times 10^{-5} \text{ einstein dm}^{-3} \text{ s}^{-1}$ was calculated.

Photocatalytic runs were carried out in a thermostated cylindrical Pyrex cell at 25°C . In all cases, a fresh 0.5 mM solution (20 cm^3) of the corresponding Hg^{II} salt was adjusted to the desired pH, the catalyst (1.0 g dm^{-3}) was suspended in the solution, and the suspension was ultrasonicated for 2 min. This catalyst concentration assures an almost complete saturation of the photocatalytic rate, according to Ref. [17]. In the presence of TiO_2 , precipitation of Hg^{II} as HgO is prevented at this concentration, even at pH 11, as will be explained later. The reaction was conducted with the reactor open to air or under a water-saturated nitrogen stream ($0.2 \text{ dm}^3 \text{ min}^{-1}$) bubbled in the suspension throughout the experiment. Prior to irradiation, suspensions were kept in the dark and stirred for 30 min, a time enough to assure substrate-surface equilibrium [8–11,17]. The extent of adsorption of Hg^{II} onto TiO_2 was determined by measuring mercuric concentrations in the filtrate (see below) before and after stirring in the dark, in the same conditions (air or nitrogen) used for irradiation. Irradiations were performed under magnetic stirring for 60 min. Samples were periodically withdrawn and filtered through $0.22 \mu\text{m}$ Millipore filters. At least, duplicated runs were carried out for each condition, averaging the results, but generally several runs were needed to assure reproducibility, especially in the presence of oxygen. In all cases, adsorption in the dark was discounted to analyze only the effect of light on the photocatalytic transformation. Changes in pH after illumination were also evaluated in the filtered

solutions. Negligible conversion (e.g., 3%, HgCl_2 , initial pH 7) was observed in the absence of TiO_2 .

Hg^{II} concentration was determined in the filtered solution by spectrophotometry at 323 nm using the KI method [27]. The detection limit of this technique is 1 ppm.

UV-Vis absorption measurements were performed with a Shimadzu 210A spectrophotometer, equipped with an integrating sphere for reflectance measurements.

The recovered photocatalyst was analyzed by X-ray diffraction (XRD) and by chemical reactions for identification of different deposits. XRD patterns were obtained at room temperature with a Philips PW-3710 diffractometer using $\text{Cu K}\alpha$ radiation. A gray deposit, soluble in concentrated nitric acid, indicated metallic Hg [25,28]. Treatment of the deposit with KI 2.5 M, giving a filtrate absorbing at 323 nm, indicated HgO [22,29].

3. Results

From the experimental data after equilibration in the dark, it can be concluded that Hg^{II} presents a good affinity for TiO_2 in all experimental conditions here considered (pH 3, 7 and 11), with adsorption percentages around 15–35%, in agreement with previous

results [8–11,14] (Fig. 1). No strong differences are seen at the different pH or in the presence or absence of oxygen.

In Fig. 2, profiles of normalized Hg^{II} concentration vs. time after UV irradiation over TiO_2 are shown. They are rather dissimilar in shape. With a few exceptions, deceleration or arrest of the reaction occurred in all systems after a certain irradiation time, with very low conversions in acid and neutral pH. Particularly, fairly good first-order kinetics was observed in all pH 11 runs; in contrast, $\text{HgCl}_2/\text{pH3}/\text{N}_2$ followed a nearly zero order kinetics.

In Fig. 3, the extent of Hg^{II} photocatalytic conversion after 60 min irradiation for each experiment is presented, taken from the smoothed curves in Fig. 2. The graph indicates an important influence of the nature of the salt and of the pH. The transformation was accompanied by a decrease of the initial pH, larger at higher conversions and in alkaline media. Except for pH 11, conversions were generally lower in the presence of oxygen, especially at pH 3. The fastest transformation took place at pH 11, although good conversions were also attained in the $\text{HgCl}_2/\text{pH7}$ (air and N_2) and $\text{HgCl}_2/\text{pH3}/\text{N}_2$ systems. The perchlorate systems attained generally slightly lower conversions. Gray (dark or pale) deposits were visually observed on the recovered photocatalyst, when conversion degrees were higher than 50% (Table 1).

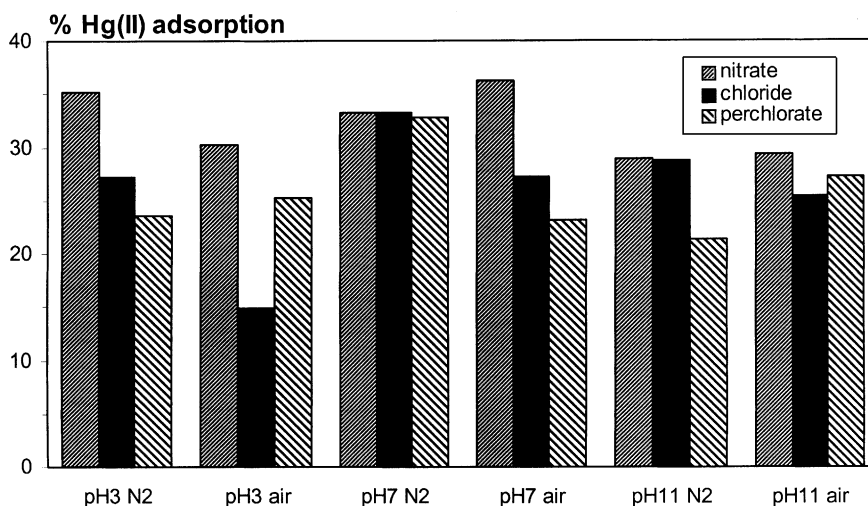


Fig. 1. Degree of adsorption of Hg^{II} salts onto TiO_2 surface at three initial pH after 30 min stirring in the dark. Conditions: $[\text{Hg}^{\text{II}}] = 0.5 \text{ mM}$, $[\text{TiO}_2] = 1 \text{ g dm}^{-3}$, $T = 25^\circ\text{C}$.

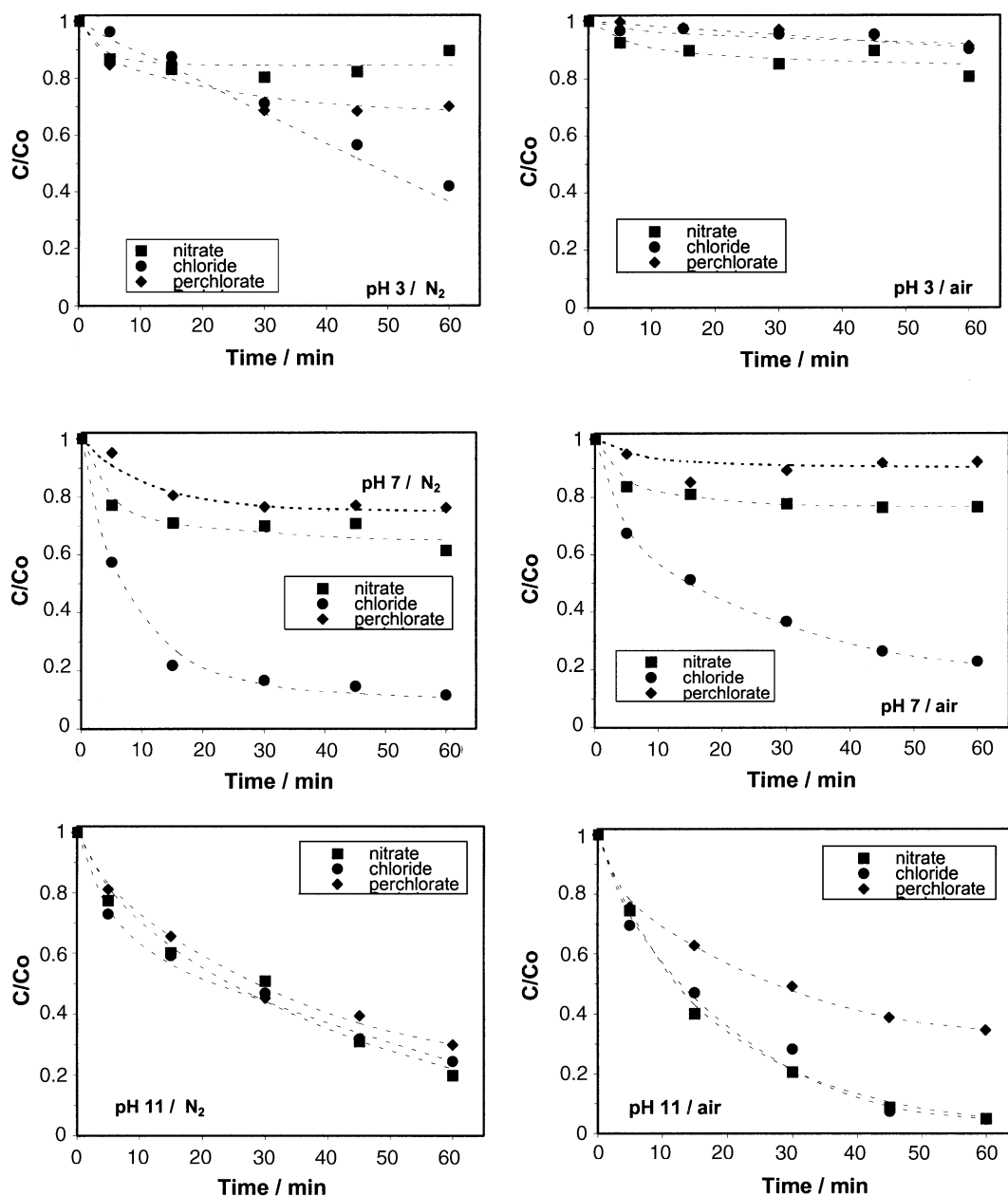


Fig. 2. Profiles of normalized Hg^{II} conversion with time at three initial pH. Conditions: $[Hg^{II}] = 0.5 \text{ mM}$, $[TiO_2] = 1 \text{ g dm}^{-3}$, $T = 25^\circ\text{C}$; near UV-light ($300 \text{ nm} < \lambda < 500 \text{ nm}$), $P_0 = 1.1 \times 10^{-5} \text{ einstein dm}^{-3} \text{ s}^{-1}$.

These deposits were analyzed chemically and by XRD, although in several cases, the low amount and the lack of crystallinity of the deposit precluded any identification. The different chemical nature of iden-

tified deposits, Hg^0 , HgO and/or calomel (Hg_2Cl_2), indicates the complexity of the system. A pale gray deposit was observed in the $HgCl_2$ systems at acid and neutral pH, identified as a mixture of Hg^0 and

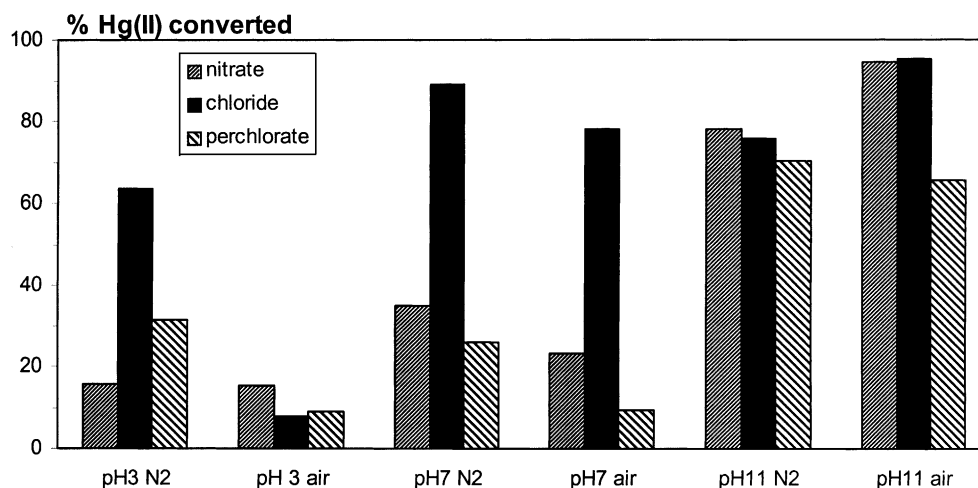


Fig. 3. Degree of Hg^{II} conversion after 60 min irradiation at three initial pH. Conditions are same as given in Fig. 2.

Table 1

Identification of the deposit on the recovered photocatalysts

Initial salt	pH	Oxygen	Type of deposit	Identified product	RX identified product
$\text{Hg}(\text{NO}_3)_2$	3	No	—	—	—
$\text{Hg}(\text{NO}_3)_2$	3	Yes	—	—	—
$\text{Hg}(\text{NO}_3)_2$	7	No	—	—	—
$\text{Hg}(\text{NO}_3)_2$	7	Yes	—	—	—
$\text{Hg}(\text{NO}_3)_2$	11	No	Dark gray	Hg, HgO	—
$\text{Hg}(\text{NO}_3)_2$	11	Yes	Dark gray	Hg, HgO	—
HgCl_2	3	No	Pale gray	Hg, Hg_2Cl_2	Hg_2Cl_2
HgCl_2	3	Yes	—	—	—
HgCl_2	7	No	Pale gray	Hg, Hg_2Cl_2	Hg_2Cl_2
HgCl_2	7	Yes	Pale gray	Hg, Hg_2Cl_2	Hg_2Cl_2
HgCl_2	11	No	Dark gray	Hg	—
HgCl_2	11	Yes	Dark gray	Hg, HgO	—
$\text{Hg}(\text{ClO}_4)_2$	3	No	—	—	—
$\text{Hg}(\text{ClO}_4)_2$	3	Yes	—	—	—
$\text{Hg}(\text{ClO}_4)_2$	7	No	—	—	—
$\text{Hg}(\text{ClO}_4)_2$	7	Yes	—	—	—
$\text{Hg}(\text{ClO}_4)_2$	11	No	Dark gray	Hg, HgO	—
$\text{Hg}(\text{ClO}_4)_2$	11	Yes	Dark gray	Hg, HgO	—

calomel. XRD analysis proved undoubtedly the presence of this compound, while it was not possible to detect Hg^0 because the peaks were masked by those of calomel. Fig. 4 shows the diffraction patterns of the recovered photocatalysts corresponding to the $\text{HgCl}_2/\text{pH}3/\text{N}_2$ (C) and $\text{HgCl}_2/\text{pH}11/\text{air}$ (B) systems, compared with pure P-25 (A). Whereas in samples (A) and (B) only peaks of anatase and rutile

phases can be seen, sample (C) exhibits clear peaks corresponding to calomel. At alkaline pH, either in air or in nitrogen, a dark gray deposit, characterized as a mixture of metallic Hg and HgO was generally formed, independently of the initial salt. Sometimes, the gray deposit was not observed, but HgO was identified by the KI test, although never detected by XRD.

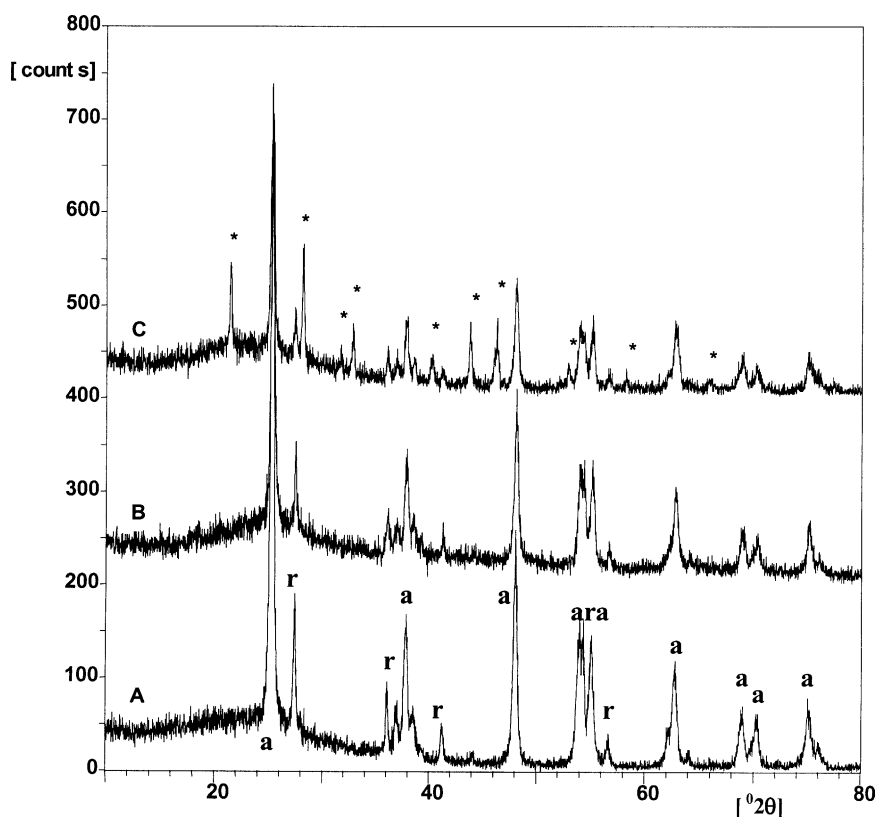


Fig. 4. XRD pattern of samples taken after HgCl_2 photocatalysis. (A) pure P-25, (B) $\text{HgCl}_2/\text{pH}11/\text{air}$, (C) $\text{HgCl}_2/\text{pH}3/\text{N}_2$ (a: anatase, r: rutile, *: calomel).

In Table 2, initial photonic efficiencies (ζ , %) are shown, calculated as

$$\zeta = \frac{(-dC/dt)_{t=0}}{P_0} \times 100 \quad (1)$$

where $(-dC/dt)_{t=0}$ is the initial reaction rate (taken from the initial slope of curves in Fig. 2) and P_0 the incident photonic flow per unit volume. Although photonic efficiencies are affected by rather large errors at the initial stages of the reaction, especially when final

conversions are very low, this parameter allows the comparison of the intrinsic reactivity of Hg^{II} in the initial conditions, independently of any deactivation, inhibition or other secondary effect that may occur at longer irradiation times. Therefore, they do not correlate strictly with conversion degrees. The values are in the order of most photocatalytic reactions in aqueous phase, around 1–4%. Slight differences in air or under nitrogen can be seen; at acid and neutral pH, efficiencies were higher in the absence of oxygen, while at pH 11 they were higher in air.

Table 2

Initial photonic efficiencies for the photocatalytic systems

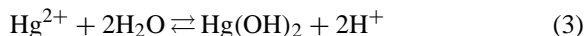
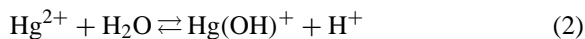
pH	Nitrate		Chloride		Perchlorate	
	N_2	Air	N_2	Air	N_2	Air
3	1.3	0.6	0.5	0.3	1.5	0.2
7	2.2	1.2	5.2	4.0	1.2	0.4
11	2.0	2.9	3.0	3.2	2.3	2.7

4. Discussion

4.1. Adsorption

Although a thorough adsorption study of mercury(II) onto TiO_2 is beyond the scope of the present

paper, some considerations can be made. Nitrate and perchlorate Hg^{II} salts are ionic, water soluble species, with a strong tendency to hydrolyze, especially at less acidic pH, according to the following equilibria:



Even at acid pH, the amount of hydroxylated species is high, e.g., at pH 3.0, $[\text{Hg}^{2+}] = [\text{Hg}(\text{OH})_2]$ [28,30]. At higher pH, polynuclear hydroxo-bridged species or basic salts such as $\text{Hg}(\text{OH})(\text{NO}_3)$ are formed [28,30,31]. HgO can be present even at pH as low as 2.4, being the stable species at pH 11 [28]. However, in the presence of TiO_2 P-25, precipitation of HgO from a 0.5 mM Hg^{II} solution is prevented because the surface of the solid becomes more acidic by adsorption of mercuric species.

Thus, the observed constancy in the adsorption can be explained by the presence of a relatively high concentration of the non-charged $\text{Hg}(\text{OH})_2$, whose adsorption is not very much altered by pH [17], in spite of changes in the surface charge of P-25 with pH ($\text{pzc} = 6.3$, [32]).

For HgCl_2 , the analysis of the adsorption is more difficult because of the covalent nature of the salt. Due to the high stabilization of Hg^{2+} , its conversion to the oxide as pH increases is less probable compared to the other two salts [28]. In addition, some hydrolytic effects take place:

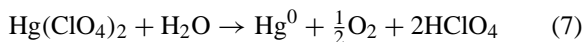
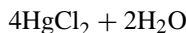
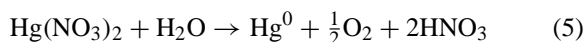


Consequently, a lower adsorption of mercuric chloride on TiO_2 could be predicted compared with that of the other two salts, due to the absence of electrostatic interactions between the species and the catalyst; however, weaker interactions (e.g., van der Waals forces) can also promote adsorption and cannot be discarded.

4.2. Photocatalytic results

4.2.1. Nature of the products

It can be proposed that the products of the global photocatalytic processes depend on the nature of the initial salt:



Note that the above equations represent processes in neutral or acid media; accordingly, a decrease of the initial pH may take place, which, although rather small, was observed in most cases. At high pH, oxidation of metallic Hg, once produced, is very rapid, particularly in the presence of oxygen [30]:

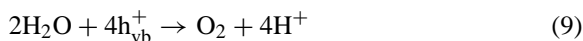


Consequently, as presented in Table 1, dark mixtures of Hg^0 and HgO were observed as deposits on the catalyst at pH 11 in the nitrate and perchlorate systems.

Calomel is observed at pH 3 and 7 in the HgCl_2 systems, together with Hg^0 , but at pH 11 only Hg and/or HgO are formed. This will be explained later.

The photocatalytic transformation of Hg^{II} has been found always strongly dependent on the reaction conditions, i.e., the nature of the mercuric salt, the presence or absence of oxygen and the initial pH (see, for example, Refs. [6,14]). We have arrived to similar conclusions, and it can be proposed that the complicated chemistry of mercury influences to a high extent the nature and rate of the photocatalytic transformation. The thermodynamic feasibility of mercury(II) transformation, after electron-hole pair generation by UV irradiation of the semiconductor, depends on the values of redox potentials of the species adsorbed onto the catalyst or close to it, in relation with the redox level of the conduction band electrons, e_{cb}^- ($V_{\text{fb}} = -0.3 \text{ V}^1$ at pH 0 [33]), the difference of potentials being the driving force for the reduction.

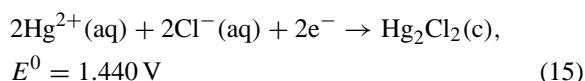
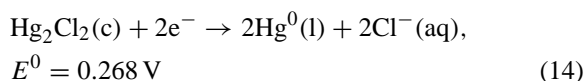
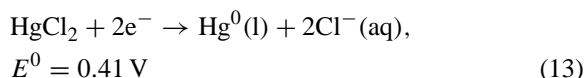
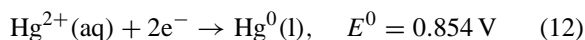
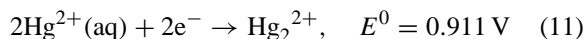
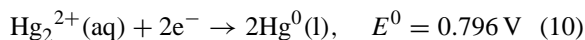
In most papers, two electron processes are proposed for the cathodic transformation of mercury(II). The concomitant anodic reaction is the oxidation of water by holes and, indeed, O_2 evolution in the mercury(II) photocatalytic system was observed in some cases [12,20]:



The redox potentials of mercury species, taken from the literature [8,9,14,34,35], are the following,

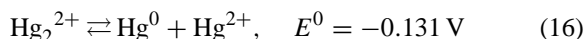
¹ All standard redox potentials cited in this work are referred to NHE.

although values at the TiO₂ interface can be somewhat different:



Based on the above values, Hg²⁺ can be reduced to both Hg₂²⁺ or Hg⁰, and Hg₂²⁺ to Hg⁰ by the same reductants (see Eqs. (10)–(12)), for example by e_{cb}[−], with similar driving forces. Although Hg²⁺ is first reduced to Hg₂²⁺, a slight excess of e_{cb}[−] or another reductant will transform Hg₂²⁺ to Hg⁰. On the other hand, reduction of Hg²⁺ to calomel seems to be thermodynamically very favorable (Eq. (15)).

However, if the process were determined only by the values of the redox potentials, reduction to metallic mercury would be less favorable for the halides, especially at less acid pH (Eqs. (13) and (14)), which is not observed in Fig. 2. Instead, it is clear that the nature of the products influences the rate and fate of the process. Nitrate and perchlorate Hg₂²⁺ salts are ionic and water soluble at acid pH, but they are unstable and disproportionate to Hg and HgO at pH > 3.5 [28]. This implies that Hg^I species, if formed in the nitrate and perchlorate systems, cannot be detected, because they will be easily transformed to Hg²⁺ [31]:



The situation is different for the chloride system because, in addition to a higher driving force for reduction of Hg^{II} to calomel by e_{cb}[−], hydrolysis and disproportion do not occur due to the high stability and insolubility of the salt; then, the reduction process stops, at least in part, at this stage. The simultaneous presence of Hg⁰ in the deposit (Table 1) can derive from the reduction of the few Hg^I ions in solution (close to the TiO₂ surface) displacing the solubility

equilibrium of Hg₂Cl₂ ($K_{\text{sp}} = 1.4 \times 10^{-18}$ [34]). However, disproportion does take place at pH > 11 [28], explaining why calomel is not observed at alkaline pH (see Fig. 4 and Table 1).

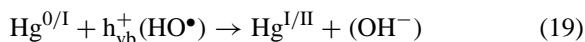
Although all previous reports suggest two electron processes for the photocatalytic reduction of Hg^{II}, the transformation might occur alternatively through two successive one-electron transfer steps:



A similar mechanism through successive one-electron steps has been proposed and demonstrated by UV-Vis and EPR spectrophotometries for the photocatalytic reduction of hexavalent chromium over TiO₂ [36,37]. In the present case, to prove the hypothesis is more difficult because mononuclear Hg⁺ species are very unstable and, due to a very small dissociation constant in water ($K_{\text{diss}} < 10^{-7}$) [34], this ion, if formed, would be rapidly transformed to the binuclear form. Mononuclear Hg⁺ species have been indeed detected by EPR and UV spectroscopies in the special cases of radiolytic reductive processes [38–40] or electrochemical oxidative dissolution of Hg⁰ by specific N-ligands [41]. They have been also proposed as intermediates in one-equivalent oxidations of the Hg^I dimer [42], in photochemical processes [43] and in photocatalytic reactions [44]. The redox potential of the couples involving the mononuclear species are not known, but if reactions (17) and (18) are considered thermodynamically possible, the one-electron mechanism can be supported by the reported existence of mononuclear species and by the fact that multielectronic processes are not likely in photocatalysis [45,46]. Although Kaluza and Boehm [7] have not detected EPR signals of paramagnetic Hg⁺ ions in the photocatalyzed oxidation of zerovalent mercury, they have suggested the intermediate occurrence of such ions. Fast photocatalytic experiments in the cavity of an EPR spectrometer are needed to demonstrate the participation of Hg⁺ ions and they will be soon performed.

On the other hand, as stated elsewhere [4,8,14,17] and proposed also for Cr^{VI} [36], reduced mercury species present on the surface of the photocatalytic particle can be reoxidized competitively by holes ($V_{\text{fb}} = +2.9 \text{ V}$ at pH 0 [33]) or by other oxidizing species such as HO• ($E^0 = +2.8 \text{ V}$ at pH 0 [2]),

formed in the cathodic route when oxygen is present (see, Eq. (24)):



These reactions are thermodynamically possible for all mercury species according to the redox potentials of reactions (10)–(15). This effect will arrest the reaction in some cases and it will be explained later. As it is not possible to oxidize Hg^0 to Hg^{I} without the concomitant oxidation to Hg^{II} , metallic Hg is directly transformed to Hg^{II} . However, in the case of the chloride system, on one hand, there is a larger driving force for oxidation of Hg^0 to calomel (reaction (14)) by holes or HO^\bullet than for calomel to Hg^{II} (reaction (15)). On the other hand, if Hg^0 is in excess, only Hg^{I} (in the form of calomel) will be present, because the metal will displace the disproportion equilibrium (16) to the left. Therefore, calomel and metallic Hg will be synergistically precipitated in the case of HgCl_2 , and this can explain the good conversion in the case of the $\text{HgCl}_2/\text{pH}7$ systems and $\text{HgCl}_2/\text{pH}3/\text{N}_2$, where Hg and calomel have been identified as deposits. Calomel can be originated also from hole attack to chloride, forming Cl^\bullet radicals, a rather powerful oxidant:



Concerning the slightly lower conversion of perchlorate systems, we do not have at this point a reliable explanation.

4.3. Influence of oxygen

Molecular oxygen can compete with Hg^{II} reduction:



Initial photonic efficiencies (Table 2) show inhibition by oxygen at acid and neutral pH, but not at pH 11 (see later). Final conversions at 60 min also agree with these results in most cases (Fig. 3), in accordance with previous works [4,8–14,16,17,19,20]. In the case of Cr^{VI} reduction, it has been proved that oxygen did not affect the photocatalytic reaction, being neither a mediator nor a competitive species; oxidation of water

by holes is here the rate limiting step [36]. In contrast, oxygen is actually a competitive species in the case of Hg^{II} , inhibiting the rate limiting cathodic step (see later), as proposed previously [8,9,16]. Additionally, oxygen is produced in the global process (see Eqs. (5)–(7)) through the anodic pathway (9), even in nitrogen purged systems. However, Domènech and Andrés [20], when using ZnO, have observed accumulation of oxygen at the initial stages of the reaction, explained by a very rapid Hg^{II} reduction that prevented the occurrence of Eq. (22). This can explain why the initial quantum efficiencies only differ slightly with or without oxygen (Table 2).

4.4. Influence of initial pH

The observed effect of the initial pH agrees very well with the results obtained by other authors [13,14,17]. The effect cannot be related to changes in adsorption, because of the relatively small differences in the studied range (see Fig. 1). Taking into account the Nernstian variation of the redox potential of TiO_2 cb electrons with pH, a lower driving force as the pH decreases could explain the poor conversion found at pH 3. However, due to hydrolytic processes, this dependence is not so strict, and the reactivity will depend also on the nature of the initial salt, related to the existence of different mercury forms either in solution or in the solid state. The low conversion rates at pH 3 and 7 (with the exception of chloride) can be interpreted mainly by Hg^0 reoxidation and/or redissolution. Metallic mercury can slowly dissolve even in diluted HNO_3 [31], and easy reoxidation of Hg_2^{2+} to $[\text{Hg}(\text{H}_2\text{O})_2]^{2+}$ species occurs in water [30]; reoxidation by holes (mentioned in the previous section) is more favorable at more acid pH. An electron shuttle mechanism comprising the sequence of reactions (17), (18) and (19) takes place continuously, as clearly seen from the dispersion of points or by plateaus after some minutes of irradiation at acid and neutral pH, especially in the presence of oxygen (Fig. 2). The case of HgCl_2 was explained in the previous section.

The high conversion at alkaline pH, also observed by Aguado et al. [17], can be due to the formation of HgO through Eq. (8), and this oxide was detected in this work at alkaline pH in most cases (Table 1). Partial oxidation of Hg photocatalytically deposited onto ZnO has been reported (pH not indicated) [20] and

HgO was observed in the photocatalytic treatment of cyanide Hg^{II} species at pH 10.5 [24]. Even in nitrogen purged systems, HgO can be produced by a higher HO^\bullet concentration coming from hole attack to the basic HO^- groups. This phenomenon has been already observed in the TiO_2 photocatalytic oxidation of Hg^0 in oxygen [7].

At these high pH, deposit of mercurous species is precluded because of easy disproportion to Hg and HgO [30],² enhanced by the presence of Hg, Eq. (16). This explains why calomel has been never detected at pH 11 (see Table 1). It also accounts for the beneficial role of oxygen at this pH, which, instead of inhibiting the reaction, helps HgO formation.

4.5. Kinetic regime

Different kinetic orders have been reported in previous studies of Hg^{II} photocatalysis, such as 0.5 [8,9] or first [17] for TiO_2 , and 7/5 for ZnO [20]. We have found a rather good first order in all systems at pH 11, in agreement with results of Aguado et al. [17], who have not tested kinetic orders at other pH. At neutral and acid pH, not a defined behavior is observed. The profiles were generally characterized by a relatively rapid initial conversion followed by a deceleration or an arrest of the rate, with the exception of $\text{HgCl}_2/\text{pH}3/\text{N}_2$, which obeys a nearly zero order. According to these results, we propose that not a single kinetic regime applies, but instead the kinetics depends on the initial conditions, the nature of the salt and the type of deposits on the photocatalyst.

We support an activation–deactivation process model, similar to the proposed and discussed in Ref. [17]. Based on the assumption that the cathodic pathway is the rate limiting step, confirmed by the negative influence of oxygen, the activation is caused by the electron trapping action of Hg deposits, which decreases recombination. This action is similar to that of Pt islands on TiO_2 [6,12], or deposits of Hg on ZnO [20], the metal decreasing the overpotential for Hg^{II} reduction. The effect is opposite to the case of Cr^{VI} photocatalytic reduction, where platinum did not exert any influence on the reaction rate [36]. Even in aerated systems, the presence of a metal on the photocatalyst

also decreases the overpotential for oxygen photoreduction to superoxide (Eq. (22)), helping separation of electron and holes. This could explain then the rather high conversion in the systems $\text{HgCl}_2/\text{pH}3/\text{N}_2$, $\text{HgCl}_2/\text{pH}7/\text{N}_2$ and $\text{HgCl}_2/\text{pH}7/\text{air}$, the only acid and neutral systems in which metallic Hg was found (Table 1). Reaction (21) can also act against recombination in the HgCl_2 systems. It seems, actually, that the reaction is enhanced as well by calomel and HgO deposits, but their action is not known.

Oppositely, after the initial stages, reoxidation of metallic Hg induces deactivation or inhibition. This is the reason why conversions at 60 min do not correlate in some cases with initial photonic efficiencies. As said before, the electron shuttle process (17)/(18) and (19) takes place continuously, especially at neutral and acid pH, which arrests the reaction. Additionally, all mercury deposits (no matter their chemical nature) can provoke deceleration by decreasing the effective irradiated TiO_2 surface and the extent of Hg^{II} adsorption, changing the nature of the TiO_2 surface and producing agglomeration of particles [13,17]. This applies to all conditions.

5. Conclusions

The nature of the mercuric species and the reaction conditions exert a strong influence in the heterogeneous photocatalytic reaction over TiO_2 . Although Hg^{II} shows a great affinity for the TiO_2 surface in the range of pH studied ((3)–(11)), there is no relationship between the photocatalytic reaction rate and the extent of adsorption. Initial pH influences considerably the reaction, the highest conversion taking place at pH 11. Some inhibition by oxygen can be observed at acid and neutral media, but not in alkaline suspensions. Gray deposits of different color intensity, composed of Hg^0 , HgO and/or Hg_2Cl_2 have been observed, depending on the initial conditions. In most cases, after a relatively high initial rate, a deceleration or arrest of the reaction is observed, attributed to redissolution and to catalyst deactivation provoked by the deposits. HgCl_2 appears distinctly different from the other two salts by the possibility of forming the stable mercurous salt. Other experiments are underway to confirm the nature of intermediates of the reaction and to evaluate the effect of the addition of organic scavengers.

² Hg_2O is not a stable species, but a mixture of Hg^0 and HgO [7,28]. Mercurous hydroxide cannot be precipitated [34].

Remediation of Hg^{II} in aqueous solutions is hard to attain completely, because of the low levels needed to avoid toxicity. Very sensitive analytical tools must be used to control the concentration of species in solution that, according to regulations, must be present only in the order of ppb. The physicochemical properties of the products derived from the treatment also introduce serious difficulties. Metallic Hg is volatile and somewhat water soluble, HgO is also fairly water soluble and the Hg^{I} and Hg^{II} nitrates and perchlorates are water soluble. Nevertheless, it will be always better to have the pollutant immobilized as a metallic deposit than leave it mobile, treating later the solid residue as a hazardous one. Zerovalent mercury can be carefully distilled off by mild heating, trapped and recondensed, as shown in Ref. [5], or it can be dissolved with nitric acid or aqua regia for confinement or further treatment of smaller volumes of the effluent. It must be also reminded that calomel is less toxic than HgCl_2 . HP, which can take advantage also of solar light, appears as a valuable tool to reduce mercury pollution in real cases to very low levels. Of course, the addition of a cooperative organic donor will improve the efficiency of the photocatalytic treatment, especially at acid pH. This action can be done by organic compounds coming in the waste waters together with mercury.

Acknowledgements

Work performed as part of Comisión Nacional de Energía Atómica CNEA-CAC-UAQ project #00Q0308 (P5 Program), Agencia Nacional de Promoción de la Ciencia y la Tecnología (ANPCYT) project PICT98-13-03672 and Consejo Nacional de Investigaciones Científicas y Técnicas (CONICET) project PIP662/98. Authors thank the CYTED Program, a “Scientific Iberoamerican Cooperation Action” (CYTED VIII-G) for subsidy. MIL is a member of CONICET.

References

- [1] M.I. Litter, *Appl. Catal. B* 23 (1999) 89.
- [2] X. Domènech, W. Jardim, M. Litter, in: M.A. Blesa (Ed.), *Eliminación de Contaminantes por Fotocatálisis Heterogénea*. Texto colectivo elaborado por la Red CYTED VIII-G, Digital Grafic, La Plata, 2001, Chapter 1, p. 3.
- [3] M. Litter, X. Domènech, H. Mansilla, in: M.A. Blesa (Ed.), *Eliminación de Contaminantes por Fotocatálisis Heterogénea*. Texto colectivo elaborado por la Red CYTED VIII-G, Digital Grafic, La Plata, 2001, Chapter 6, p. 121.
- [4] N. Serpone, E. Borgarello, E. Pelizzetti, in: M. Schiavello (Ed.), *Photocatalysis and Environment*, Kluwer Academic Publishers, Dordrecht, 1988, p. 527.
- [5] L.D. Lau, R. Rodríguez, S. Henery, D. Manuel, *Environ. Sci. Technol.* 32 (1998) 670.
- [6] P. Clechet, C. Martelet, J.-R. Martin, R. Olier, *C.R. Acad. Sci., Paris Ser. B* 287 (1978) 405.
- [7] U. Kaluza, H.P. Boehm, *J. Catal.* 22 (1971) 347.
- [8] M.R. Prairie, L.R. Evans, S.L. Martínez, *Chem. Oxid.* 2 (1992) 428.
- [9] M.R. Prairie, L.R. Evans, B.M. Stange, S.L. Martínez, *Environ. Sci. Technol.* 27 (1993) 1776.
- [10] M.R. Prairie, B.M. Stange, *AIChE Symp. Ser.* 89 (1993) 460.
- [11] M.R. Prairie, B.M. Stange, L.R. Evans, in: D.F. Ollis, H. Al-Ekabi (Eds.), *Photocatalytic Purification and Treatment of Water and Air*, Elsevier, Amsterdam, 1993, p. 353.
- [12] K. Tanaka, K. Harada, S. Murata, *Sol. Energy* 36 (1986) 159.
- [13] J. Domènech, M. Andrés, *Gazz. Chim. Ital.* 117 (1987) 495.
- [14] N. Serpone, Y.K. Ah-You, T.P. Tran, R. Harris, E. Pelizzetti, H. Hidaka, *Sol. Energy* 39 (1987) 491.
- [15] A. Hilmi, J.H.T. Luong, A.-L. Nguyen, *Chemosphere* 38 (1999) 865.
- [16] D. Chen, A.K. Ray, *Chem. Eng. Sci.* 56 (2001) 1561.
- [17] M.A. Aguado, S. Cervera-March, J. Giménez, *Chem. Eng. Sci.* 50 (1995) 1561.
- [18] J. Bussi, M. Chanian, M. Vázquez, E.A. Dalchiele, *J. Environ. Eng.* 128, in press.
- [19] J. Domènech, M. Andrés, J. Muñoz, *Tecnol. Agua* 29 (1986) 35.
- [20] J. Domènech, M. Andrés, *New J. Chem.* 11 (1987) 443.
- [21] Z.-H. Wang, Q.-X. Zhuang, *J. Photochem. Photobiol. A* 75 (1993) 105.
- [22] K. Tennakone, C.T.K. Thaminimulle, S. Senadeera, A.R. Kumarasinghe, *J. Photochem. Photobiol. A* 70 (1993) 193.
- [23] L.X. Chen, T. Rajh, Z. Wang, M.C. Thurnauer, *J. Phys. Chem. B* 101 (1997) 10688.
- [24] W.S. Rader, L. Solujic, E.B. Milosavljevic, J.L. Hendrix, J.H. Nelson, *J. Sol. Energy Eng.* 116 (1994) 125.
- [25] K. Tennakone, U.S. Ketippearachchi, *Appl. Catal. B* 5 (1995) 343.
- [26] C.G. Hatchard, C.A. Parker, *Proc. R. Soc. A* 235 (1956) 518.
- [27] A.J. Pappas, H.B. Powell, *Anal. Chem.* 39 (1967) 579.
- [28] F.B. Martí, F.L. Conde, S.A. Jimeno, *Química Analítica Cualitativa*, Paraninfo, Madrid, 1994, p. 435.
- [29] I.M. Kolthoff, E.B. Sandell, E.J. Meehan-Stanley Bruckenstein, *Análisis Químico Cuantitativo*, Nigar, Buenos Aires, 1969, p. 808.
- [30] F.A. Cotton, G. Wilkinson, *Química Inorgánica Avanzada*, Limusa, México, 1998, p. 715.
- [31] N.N. Greenwood, A. Earnshaw, *Chemistry of the Elements*, Butterworths/Heinemann, Oxford, 1997, p. 1201.
- [32] D. Bahnemann, J. Cunningham, M.A. Fox, E. Pelizzetti, P. Pichat, N. Serpone, in: G.R. Helz, R.G. Zepp, D.G. Crosby (Eds.), *Aquatic and Surface Photochemistry*, Lewis Publishers, Boca Raton, FL, 1995, p. 261.

- [33] S.T. Martin, H. Herrmann, M.R. Hoffmann, *J. Chem. Soc., Faraday Trans.* 90 (1994) 3323.
- [34] J. Balej, in: A.J. Bard, R. Parsons, J. Jordan (Eds.), *Standard Potentials in Aqueous Solution*, Marcel Dekker, New York, 1985, Chapter 10, p. 265.
- [35] R.C. Weast (Ed.), *Handbook of Chemistry and Physics*, CRC Press, Boca Raton, FL, 1980–1981, p. D-158.
- [36] U. Siemon, D. Bahnemann, J.J. Testa, D. Rodríguez, N. Bruno, M.I. Litter, *J. Photochem. Photobiol. A: Chem.* 148 (1–3) (2002) 247–255.
- [37] J.J. Testa, M.A. Grela, M.I. Litter, *Langmuir* 17 (2001) 3515.
- [38] R.S. Eachus, F.G. Herring, *Can. J. Chem.* 49 (1971) 2868.
- [39] M.N. Grecu, *Rev. Roum. Phys.* 36 (1991) 875.
- [40] N.S. Dalal, D. Netti, P. Grandinetti, *J. Am. Chem. Soc.* 104 (1982) 2054.
- [41] A. Renuka, K. Shakuntala, P.C. Srinivasan, *Indian J. Chem.* 37A (1998) 596.
- [42] R. Davies, B. Kipling, A.G. Sykes, *J. Am. Chem. Soc.* 95 (1973) 7250.
- [43] V. Balzani, V. Carasiti, *Photochemistry of Coordination Compounds*, Academic Press, London, 1970, p. 276.
- [44] E.C. Dutoit, F. Cardon, W.P. Gomes, *Ber. Bunsen-Gesellsch.* 80 (1976) 1285.
- [45] B.R. Müller, S. Majoni, R. Memming, D. Meissner, *J. Phys. Chem. B* 101 (1997) 2501.
- [46] M.A. Grela, A.J. Colussi, *J. Phys. Chem.* 100 (1996) 18214.